RICE UNIVERSITY

MEASUREMENTS ON SUPERSONIC PLASMA FLOW IN A DIVERGING CHANNEL

by

Kenneth Porter Horn

A THESIS SUBMITTED
IN PARTIAL FULFILLMENT OF THE
REQUIREMENTS FOR THE DEGREE OF
MASTER OF SCIENCE

May 15, 1962
Allen J. Chapman

Houston, Texas
May, 1962

ABSTRACT

The isolated effect of divergence angle on nozzle performance and the variation of nozzle performance over a wide range of divergence angles are determined. Data for nozzles with area ratio of 200, which vary in conical half angle from 10 to 45 degrees, are included. An analytical expression is developed which explains the test results. Since the flow is partially ionized, the effect of catalytic and non-catalytic wall materials on nozzle performance is also investigated.

ACKNOWLEDGEMENT

This investigation was sponsored by Project SQUID which is supported by the Office of Naval Research, Department of the Navy, under Contract No. NORM-1858(25) and by the National Aeronautics and Space Administration Grant NsG-3-59.

The author wishes to express his appreciation to Dr. A. J. Chapman and Dr. H. K. Beckmann for their guidance during the course of this work.

TABLE OF CONTENTS

INTRODUCTION

By adding the supersonic section to a thrust nozzle the thrust output is theoretically increased. For un-ionized monatomic gas flow, 80% of the theoretical maximum thrust is produced in the convergent section and only 20% in the divergent section. However, for initially fully ionized monatomic gas flow, as much as 50% of the theoretical maximum thrust can be produced in the divergent section.[1] Thus, in the latter case the increase in thrust due to the divergent section over the convergent section may be as much as 100%. Actually, such an increase is not obtained in practice because of losses present. These losses include friction, velocity misalignment, turbulence, non-uniformity of properties, and heat transfer to walls. For low density flow at high temperature these losses become very significant.

This investigation is concerned with high energy flow of helium at a stagnation pressure of approximately atmospheric pressure exhausting into a near vacuum through a supersonic nozzle. The effect of divergence angle on the performance of the nozzle is examined for the particular case of constant area ratio.

SYMBOLS

C_F	thrust coefficient
D	hydrodynamic drag
$\overline{C_D}$	average draf coefficient
F	thrust
A	cross sectional area
S	surface area
P	pressure
ρ	density
U	velocity
q	dynamic pressure
μ	viscosity
ν	kinematic viscosity
r	cross sectional radius
P_a	back pressure
u,v	velocity components in x- and y-direction
$\dot{m}$	mass flow rate
x	distance along axis
T	absolute temperature
$\overline{T}$	reference temperature in boundary layer
R	Reynolds number
M	Mach number
τ_o	shear at wall
R	$(N_{PR})^{1/2}$
N_{PR}	Prandtl number
c_f	local skin friction coefficient
θ	cone half angle
C_1	Sutherland constant
γ	ratio of specific heats
L	characteristic length
m	exponent in $U \propto x^m$
f"(0)	velocity gradient at wall

Subscripts:

ex	nozzle exit
x	axial direction
o	stagnation state
s	wall

Superscripts:

*	throat state

EXPERIMENTAL APPARATUS

The series of tests were performed in The Rice University's supersonic wind tunnel. A high stagnation enthalpy was obtained by using a plasma arc chamber powered by a 50 kw d.c. arc welding generator. This high energy was used to partially ionize helium gas. Figure 1 shows the general schematic drawing of the plasma facility. A model HF 20-1-W Miller high frequency starter was employed to initially ionize the gas so that the arc could be struck. The arc chamber assembly was mounted on a pneumatic lift, which was used to raise the chamber into the test section. The test section was connected to a 1000 cubic foot vacuum sphere, which was kept at a pressure below 100 microns of mercury absolute by means of a mercury diffusion pump. A solenoid valve was placed in the line between the supply cylinder and the flow orifice. The flow was metered with a 0.025 inch diameter orifice. The resulting mass flow rate was 0.123 grams of helium per second. A Minneapolis-Honeywell Visicorder was employed to record the other measured quantities, since this recorder combined the convenience of direct recording instruments with the sensitivity characteristics of photographic type oscillographs.

Figure 2 shows a drawing of the arc chamber assembly. The electric arc was struck between two thoriated tungsten

electrodes which were mounted in copper holders. These holders acted as heat sinks. The upper electrode (cathode) served also as the converging section of the nozzle. The throat diameter was approximately one eighth of an inch. The bottom electrode (anode) had a small hole drilled in it to allow for measurement of the stagnation pressure. A Statham strain gage pressure transducer was used to measure this stagnation pressure. It was calibrated by sealing off the throat area of the upper electrode and then applying a known pressure from the helium cylinder. The gap spacing between the two electrodes was kept at 0.10 inches. The helium was injected tangentially into the arc chamber between the electrodes. This resulted in vortex flow which helped to stabilize the arc. The negative arc voltage lead was wrapped in a coil around the upper electrode. The resulting magnetic field produced by this coil tended to rotate the arc. Thermocouples were mounted to the two electrode holders to record the temperature change during a test. This permitted an estimation of the heat transfer loss and the efficiency of the system. The electrodes were separated by a teflon spacer, which had a boron nitride insert constructed in the spacer. This insert formed the actual inside wall of the arc chamber.

The thrust was measured by means of a lever system as shown in Figure 3. The arc chamber assembly and nozzle were mounted on one side of the lever arm and a Statham strain gage load cell on the other. A lead counterweight was also mounted on the load cell side to help balance the lever arm. The arc voltage leads were brought in at the fulcrum of the lever, thereby contributing no external force on the system. A viscous damper was installed on the arc chamber side of the lever arm to damp out vibrations. The thrust was calibrated before each test by placing a known weight on the nozzle and recording its deflection on the recorder.

Two different nozzles were fabricated. They were similar except for nozzle material. One was constructed of aluminum with a copper insert at the throat, while the other was constructed of teflon with a boron nitride insert. Figure 4 shows a scale drawing of the nozzle. The throat diameter was 0.125 inches, and was made to mate the throat cut in the upper electrode. An O-ring was set into the insert to prevent leakage of gas between the convergent and divergent sections of the nozzle. The area ratio of the divergent section remained 200 during all tests.

PROCEDURE

Preliminary tests were conducted to obtain a suitable nozzle area ratio. A conical divergent nozzle with a fixed half angle of thirty degrees and an area ratio of 730 was constructed. Tests corresponding to different area ratios were conducted until the area ratio was reduced to unity. From these tests an optimum area ratio, based on thrust coefficient, of two hundred was selected.

Using this area ratio a series of tests were performed on the aluminum nozzle to determine the effect of the half angle on the nozzle performance. The half angle was varied from 10 to 45 degrees in 2 1/2 degree increments. Another nozzle, constructed of teflon, was tested with half angles of 32 1/2 and 35 degrees.

Because of the high temperature produced in the arc chamber, the duration of a test was kept to one half second. Therefore, a time sequencing system had to be employed to control automatically the necessary events of such a test. After the test section was evacuated, the helium supply pressure was selected to obtain the desired mass flow rate, and the zero readings on the oscillograph were recorded, the test was automatically controlled.

The oscillograph recorded arc voltage, arc current, stagnation pressure, bottle supply pressure, thrust, upper and lower electrode temperatures, and test length.

THEORY

The over-all performance of a thrust nozzle can be expressed in terms of the thrust coefficient. The thrust coefficient, C_F, is defined as the thrust divided by the stagnation pressure and the throat area. A theoretical thrust coefficient expression will now be derived, which will include corrections for losses due to hydrodynamic drag and velocity misalignment or obliquity. This equation will be written as a function of the conical half angle.

Hydrodynamic drag results from a shear stress acting on the nozzle wall. This shear stress is due to the viscosity of the fluid. In any real fluid the fluid velocity varies from zero at the wall to a free stream value some distance from the wall. Even with small viscosities the shear stress near the wall may be considerable because of the large velocity gradient normal to the flow. This physical picture suggests the concept of the boundary layer in which the fluid is assumed to be viscous near the wall and inviscid away from the wall, in the potential core. The boundary layer extends from the wall to a distance where the fluid velocity is some set percent of the free stream velocity. This concept of a boundary layer can be applied to the flow in a channel only if the boundary layer remains

thin relative to the width of the channel. If the boundary layer does not remain thin, the assumption of a potential core is violated. As the boundary layer grows a point in the flow is reached at which the layers from the opposite walls interfer, and the flow becomes "fully developed" laminar flow.

Consider the nozzle shown below in Figure A.

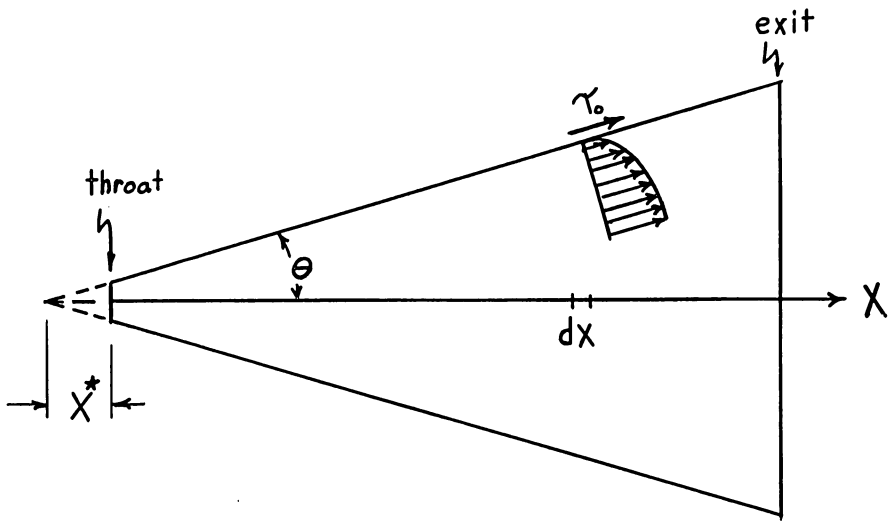

Figure A. Illustrating the calculation of skin friction on a nozzle wall.

The viscous drag for this case of flow through a nozzle becomes,

$$D = \int \cos\theta \, \tau_o \, dS = \cos\theta \int c_f \, \tfrac{1}{2} \rho u^2 \, dS \qquad (1)$$

where θ is the half angle of the nozzle and c_f is the

local skin friction coefficient. In order to calculate c_f it is necessary to know the velocity gradient at the wall of the nozzle. This can be found by the solution of the differential equations of the boundary layer. Flow through a nozzle is a case of axi-symmetric flow. The results of boundary layer calculations for plane flow can be applied to axi-symmetric flow if the set of transformations, devised by W. Mangler[10], are used.

Since the flow in a nozzle has a non-zero pressure gradient, the usual boundary layer solution of laminar flow over a flat plate of zero incidence cannot be applied. However, in the case of wedge flow, the boundary layer equations are given by,

$$u \frac{\partial u}{\partial x} + v \frac{\partial u}{\partial y} = U \frac{dU}{dx} + \nu \frac{\partial^2 u}{\partial y^2}$$

$$\frac{\partial u}{\partial x} + \frac{\partial v}{\partial y} = 0 \quad .$$

The solution of this problem was first deduced by V. M. Falkner and S. W. Skan[5]. In their solution of flow past a wedge, the velocity of the potential core was assumed to be proportional to a power of the length measured from the apex. Since the velocity in the divergent section of a nozzle can be represented by such a power of the length co-ordinate, then the local skin friction coefficient found for wedge flow can be used, or,

$$c_f = 2 f''(0) \sqrt{m+1}\ R^{-1/2}, \qquad (2)$$

where m is the power of the length co-ordinate in $U \propto l^m$ and f''(0) is the dimensionless velocity gradient at the wall. For this case of flow past a wedge f''(0) is a function of m.

The Reynolds number may be written as $R = \dot{m}\, x/A \mu \cos\theta$ cos θ since by the continuity equation, $\dot{m} = \rho A u$. Also, for a conical channel the area at any cross section can be written in terms of the length co-ordinate and the conical half angle, or

$$A = \pi r^2 = \pi \tan^2\theta \cdot x^2 \qquad (3)$$

The thrust at any cross section can be written as,

$$F = A(P + \rho u^2) = A(P + 2q)$$

$\simeq$ A2q. since the static pressure term is small compared to the corresponding dynamic pressure term at any distance away from the throat. Since most of the available theoretical thrust is produced in the convergent section of the nozzle even for a slightly ionized gas, then F can be set equation to F*, the thrust at the throat, without introducing much error, so that

$$F^* = 2 A q_1 \quad . \tag{4}$$

q is the average $1/2\,\rho u^2$ at any cross section in the supersonic section of the nozzle.

Substituting (2), (3), (4) into (1) yields,

$$D = \int_0^{x_{ex}} c_f F^* \cot\theta \; x^{-1} \, dx$$

$$= \left(\frac{\pi}{m}\right)^{1/2} F^* \int_0^{x_{ex}} 2 f''(0) \sqrt{m+1} \; \mu^{1/2} \; x^{-1/2} \, dx \quad . \tag{5}$$

The viscosity is a function of the square root of the temperature by Sutherland's formula[3]. At high velocities it is necessary to include the effect of the variation of viscosity in the boundary layer. On an empirical basis Eckert[4] recommends that the viscosity be evaluated at a reference temperature in the boundary layer, or

$$\bar{T} = T + 1/2\,(T_s - T) + 0.22\, R\,(\gamma - 1)\, M^2\, T/2 \tag{6}$$

or,

$$\bar{T}/T = 1/2\; T/T_o + 1/2\; T_s/T_o + 0.22\, R\,(1 - T/T_o) \tag{7}$$

where R is the recovery factor and is given by

$$R = (N_{PR})^{1/2} \quad .$$

The viscosity can then be expressed in terms of the reference temperature by,

$$\mu = C_1 \cdot T^{1/2} \quad . \tag{8}$$

Substituting (8) into (5) gives,

$$D = F^* \left(\frac{\pi C_1}{\dot{m}}\right)^{1/2} \int_0^{x_{ex}} 2 f''(0) \sqrt{m+1}\ \bar{T}^{1/4}\ x^{-1/2}\, dx \quad ,$$

and if a dimensionless length co-ordinate, (x/x*), is introduced then,

$$D = \cot^{1/2}\theta \left[F^*\, T_o^{1/4}\, (A^* \pi)^{1/4}\, (C_1/\dot{m})^{1/2} \cdot \int_1^{(x/x^*)_{ex}} 2 f''(0) \sqrt{m+1}\, \left(\frac{\bar{T}}{T_o}\right)^{1/4} \left(\frac{X}{X^*}\right)^{-1/2} d\left(\frac{X}{X^*}\right) \right] \quad . \tag{9}$$

Finally, then, the hydrodynamic drag may be written as

$$D = [\ldots]\ \cot^{1/2}\theta \quad , \tag{10}$$

where the bracket, [. . . .], includes constants in (9), determined for given flow conditions, and the value of the integral. The integral can be evaluated since $f''(0) \cdot (m+1)^{1/2}$ and $\bar{T}/T_o$ can be expressed in terms of (x/x*).

"Velocity misalignment," or obliquity, refers to the decrease in momentum due to a velocity component normal to the nozzle axis. If it is assumed that the streamlines are concentric cones diverging from the cone apex and that the velocities are normal to the spherical cap formed at the nozzle exit, then the x-component of the total momentum can be expressed by[7],

$$\dot{m}\ u\ (1 + \cos\theta)/2 \quad . \tag{11}$$

The net thrust coefficient can be defined as,

$$C_F = F_{net} / P_o A^* \quad . \tag{12}$$

By considering the static equilibrium equation and the momentum equation for one dimensional flow through a nozzle, the nonviscous thrust can be represented by,

$$F = \dot{m}\, u_{ex} + A_{ex} (P_{ex} - P_a) \tag{13}$$

and $F = \dot{m}\, u_{ex}$, if the pressure difference term is neglected.

If the viscous effects are included, the net thrust is reduced by the amount of the drag acting in the axial direction. Therefore,

$$F_{net} = \dot{m}\, u_{ex} - D \quad . \tag{14}$$

Finally, if the value for D obtained in equation (10) and the correction for velocity obtained in equation (11) are combined with equation (12), then the net thrust coefficient can be expressed by,

$$C_F = \dot{m}\, u_{ex} \left(\frac{1 + \cos\theta}{2}\right) / P_o A^* - [\cdots] \cot^{1/2}\theta. \tag{15}$$

Equation (15) is a theoretical thrust coefficient expression which is expressed as a function of the conical half angle.

DISCUSSION

The thrust coefficient is a measure of the performance of a thrust nozzle. The values of thrust coefficient determined from the test data using the aluminum nozzle are shown in Figure 6 plotted against conical half angle. The vertical lines represent the range of values measured for a given test. The largest value of thrust coefficient corresponded to a conical half angle of 35 degrees.

The hydrodynamic drag expression derived in the Theory section assumed a local skin friction coefficient based on theoretical results of boundary layer theory. This approach was used, since empirical skin friction coefficient data for compressible flows with pressure gradients are very scarce. The solution of the boundary layer equation for high velocity compressible flow is very difficult, since in the determination of the skin friction coefficient four new parameters must be considered:

1) Viscosity function, μ (T)
2) Mach number
3) Prandtl number
4) Heat transfer.[10]

In the theoretical approach considered in the preceding section only one of these four quantities was included, that of viscosity as a function of boundary layer temperature. It has been found, however, that the skin friction coefficient

depends only weakly on the Mach number, and the effect of the Prandtl number is almost negligible[12]. The equation for the theoretical thrust coefficient (equation 15) was solved by using isentropic gas tables for helium and by assuming average test conditions of $\dot{m}$ = 0.123 grams of helium per second, P_o = 15 psia, and T_o = 27,500 ^oR.

Figure 5 shows this curve plotted as a function of conical half angle and average Reynolds number. This curve exhibited the same general shape as the experimentally determined curve. For small angles the thrust coefficient was low because of the large drag force; for very large half angles the thrust coefficient was low because of the small component of the velocity in the axial direction. The optimum half angle was 36 degrees. Figure 7 shows a comparison of the theoretical and experimental values. Since only two losses were considered in the theoretical approach, it is reasonable that the theoretical values should be greater than the corresponding experimental ones.

An average drag coefficient, $\overline{C_D}$, was determined from the test data for each half angle, since

$$C_F = F/P_o A^* - K \overline{C_D} \cot \theta$$

where K was the product of the average dynamic pressure and the surface area, and by disregarding the viscous effects the thrust was found using isentropic tables for an area

ratio of 200. A plot of $\overline{C_D} \cdot \overline{R}^{1/2}$ as a function of half angle is shown in Figure 8. This product is almost constant, thus implying $\overline{C_D}$ is a function of Reynolds number only. Thus the effect of Mach number, Prandtl number, and heat transfer on skin friction coefficient are small in this particular case.

Tests were conducted using the teflon nozzle over a limited range of half angles (Figure 9). No noticeable change in results were detected. This implied that the nozzle wall material, whether catalytic or not, did not influence the performance of the thrust nozzle at high temperature flow.

SUMMARY OF RESULTS

The following results were obtained:

1. For the given nozzle area ratio, the optimum nozzle performance corresponded to a conical half angle of approximately thirty-five degrees.
2. For this particular case of supersonic plasma flow in a diverging nozzle, the average drag coefficient can be expressed by the laminar law of friction.
3. For the given test conditions, the momentum losses were not a function of the wall material.

REFERENCES

1. Beckmann, H. K. and Chapman, A. J., "Thrust from Partly Ionized Monatomic Gases," Journal of the American Rocket Society (forthcoming).

2. Bray, K. N. C., "Atomic Recombination in a Hypersonic Wind-Tunnel Nozzle," Journal of Fluid Mechanics, Vol. 6, Part 1, July, 1959.

3. Chapman, A. J., Heat Transfer, Macmillan Co., New York, 1960.

4. Crocco, L., "One-Dimensional Treatment of Steady Gas Dynamics," Fundamentals of Gas Dynamics, Vol. III, Princeton University Press, Princeton, 1958.

5. Eckert, E. R. G., "Engineering Relations for Friction and Heat Transfer to Surfaces in High Velocity Flow," Journal of the Aeronautical Sciences, Vol. 22, 1955.

6. Falkner, V. M. and Skan, S. W., "Some Approximate Solutions of the Boundary Layer Equations," Philosophical Magazine, Vol. 12, 1931.

7. Farley, J. M. and Campbell, C. E., "Performance of Several Methods-of-Characteristics Exhaust Nozzles," NASA TN-D293, 1960.

8. Hartree, D. R., "On an Equation in Falkner and Skan's Approximate Treatment of the Equations of the Boundary Layer," Proceedings of the Cambridge Philosophical Society, Vol. 33, Part II, 1937.

9. Keenan, J. H. and Kaye, J., Gas Tables, John Wiley and Sons, New York, 1957.

10. Schlichting, H., Boundary Layer Theory, 4th ed., McGraw-Hill, New York, 1960.

11. Sears, F. W., An Introduction to Thermodynamics, The Kinetic Theory of Gases, and Statistical Mechanics, Addison-Wesley, Reading, 1959.

12. Shapiro, A. H., The Dynamics and Thermodynamics of Compressible Fluid Flow, Vols. I and II, Ronald Press, 1953.

13. Steffen, F. W., Krull, H. G., and Schmiedlin, R. F., "Effect of Divergence Angle on the Internal Performance Characteristics of Several Conical Convergent-Divergent Nozzles," NASA RM E54H25, 1954.

EXPERIMENTAL DATA

Table 1

Test No.	Nozzle expression angle (degrees)	Stagnation Pressure (psia)	Thrust (grams)	Power Input (KW)	C_f
1	10	23.2	82	27.8	0.64
		19.6	59	23.9	0.54
2	10	19.2	66	32.8	0.62
		18.9	57	43.0	0.54
3	10	17.0	61	20.5	0.64
		17.6	57	35.8	0.58
4	12 1/2	14.1	54	19.9	0.68
		16.2	44	31.2	0.49
5	12 1/2	16.6	54	36.6	0.58
		17.4	56	42.0	0.58
6	12 1/2	15.0	56	35.4	0.67
		15.6	52	40.5	0.60
7	15	18.0	74	25.4	0.74
		18.7	78	32.3	0.72
8	15	20.5	82	31.5	0.72
		19.6	67	38.2	0.61
9	15	19.9	74	44.0	0.67
		19.7	72	39.3	0.66
10	17 1/2	17.5	76	23.5	0.78
		15.8	65	19.0	0.74
11	17 1/2	16.8	76	19.3	0.82
		16.0	59	37.6	0.66
12	17 1/2	18.4	73	24.7	0.71
		16.8	65	21.8	0.69
13	17 1/2	15.4	59	33.4	0.69
		16.7	59	55.0	0.63
14	17 1/2	17.7	69	22.7	0.70
		14.9	53	32.6	0.63
15	20	19.7	84	34.7	0.77
		21.2	86	37.4	0.73
16	20	21.1	91	34.3	0.78
		21.7	79	37.8	0.66
17	20	21.1	91	34.3	0.77
		22.0	79	37.8	0.65
18	22 1/2	18.6	80	34.0	0.77
		18.8	78	33.4	0.75
19	22 1/2	18.8	85	35.5	0.81
		19.3	80	36.2	0.75
20	22 1/2	19.7	88	32.7	0.81
		20.1	83	33.8	0.75

Test No.	Nozzle expression angle (degrees)	Stagnation Pressure (psia)	Thrust (grams)	Power Input (KW)	C_f
21	22 1/2	19.7	90	34.0	0.83
		20.1	88	34.3	0.79
22	22 1/2	18.8	87	32.8	0.84
		19.0	85	33.8	0.81
23	25	17.3	86	37.5	0.90
		17.3	82	36.7	0.85
24	25	15.5	76	35.0	0.87
		15.8	69	43.3	0.79
25	25	15.6	73	38.2	0.84
		15.4	64	46.4	0.81
26	25	19.0	87	33.4	0.83
		20.6	87	39.0	0.77
27	27 1/2	18.2	86	34.6	0.85
		18.1	84	33.1	0.84
28	27 1/2	17.7	86	35.8	0.88
		17.5	84	35.9	0.86
29	27 1/2	17.8	88	35.4	0.89
		17.5	80	36.2	0.82
30	30	13.7	65	40.4	0.86
		13.4	61	35.2	0.83
31	30	14.6	71	37.1	0.88
		14.3	69	37.1	0.87
32	30	13.4	63	37.9	0.85
		14.0	63	41.5	0.82
33	30	13.4	67	36.6	0.90
		13.4	65	39.0	0.88
34	30	14.7	68	42.2	0.83
		14.8	68	37.0	0.82
35	32 1/2	13.9	70	33.4	0.90
		14.1	66	38.7	0.84
36	32 1/2	14.3	74	38.4	0.93
		14.1	72	37.1	0.90
37	32 1/2	13.9	67	35.4	0.86
		13.4	61	38.4	0.82
38	32 1/2	14.3	70	37.4	0.89
		14.1	67	39.7	0.85
39	35	14.4	74	33.1	0.93
		14.5	72	38.0	0.90
40	35	14.4	72	38.0	0.91
		14.3	67	35.0	0.84
41	35	13.7	71	35.9	0.93
		13.8	67	40.0	0.87
42	35	14.7	74	38.8	0.91
		14.6	70	38.4	0.87

Test No.	Nozzle expression angle (degrees)	Stagnation Pressure (psia)	Thrust (grams)	Power Input (KW)	C_f
43	37 1/2	14.3	70	36.8	0.90
		13.9	66	38.4	0.86
44	37 1/2	14.3	72	39.1	0.91
		14.6	72	37.6	0.89
45	37 1/2	14.3	70	37.8	0.89
		14.6	70	36.6	0.87
46	40	15.0	70	36.2	0.84
		14.7	65	37.6	0.80
47	40	15.1	70	34.2	0.83
		15.0	66	36.8	0.79
48	40	14.8	71	35.4	0.86
		14.7	67	36.7	0.82
49	40	15.2	73	34.7	0.86
		15.2	71	39.3	0.85
50	42 1/2	15.0	65	34.6	0.77
		15.1	62	35.6	0.74
51	42 1/2	15.1	70	36.7	0.84
		15.3	68	40.2	0.81
52	42 1/2	15.1	68	38.3	0.82
		15.0	66	40.0	0.80
53	42 1/2	14.7	66	36.3	0.81
		14.3	62	38.8	0.78
54	45	15.0	67	30.5	0.80
		15.3	67	33.0	0.76
55	45	15.0	65	35.3	0.78
		15.1	65	34.6	0.78
56	45	14.9	67	36.4	0.81
		15.1	67	36.0	0.80
57	45	15.4	67	36.3	0.78
		15.2	65	34.7	0.77
101	32 1/2	14.5	68	35.9	0.84
		14.3	65	38.3	0.82
102	32 1/2	14.7	68	35.8	0.83
		14.5	65	40.5	0.81
103	32 1/2	14.6	65	34.6	0.80
		14.6	63	33.0	0.78
104	32 1/2	15.2	73	38.2	0.87
		15.3	71	37.6	0.84
105	35	14.5	67	33.1	0.83
		15.1	67	33.1	0.80
106	35	15.2	76	36.4	0.90
		15.3	76	35.9	0.89
107	35	14.5	71	17.6	0.89
		15.2	71	33.4	0.85
108	35	15.0	73	36.3	0.88
		15.2	71	35.3	0.85

CALCULATED DATA

Table 2

θ	$\frac{F}{P_o A^*}\left(\frac{1+\cos\theta}{2}\right)$	$[\cdots]\cot^{\frac{1}{2}}\theta$	$C_{F_{th}}$	$C_{F_{exp.}}$	$\bar{R}$	$\sqrt{\bar{R}}$	$\bar{C}_D$	$\bar{C}_D \cdot \bar{R}^{1/2}$	L/D
10	1.603	0.967	0.636	0.59	372	19.3	0.098	1.9	11.34
15	1.587	0.785	0.802	0.68	246	15.7	0.134	2.1	7.46
20	1.566	0.675	0.891	0.72	180	13.4	0.169	2.3	5.49
25	1.539	0.598	0.941	0.83	142	11.9	0.180	2.1	4.29
30	1.507	0.535	0.972	0.86	115	10.7	0.216	2.3	3.46
35	1.469	0.486	0.983	0.90	94.3	9.72	0.220	2.1	2.86
40	1.426	0.444	0.982	0.83	80.5	8.97	0.270	2.4	2.38
45	1.378	0.407	0.971	0.79	66.0	8.12	0.317	2.6	2.00

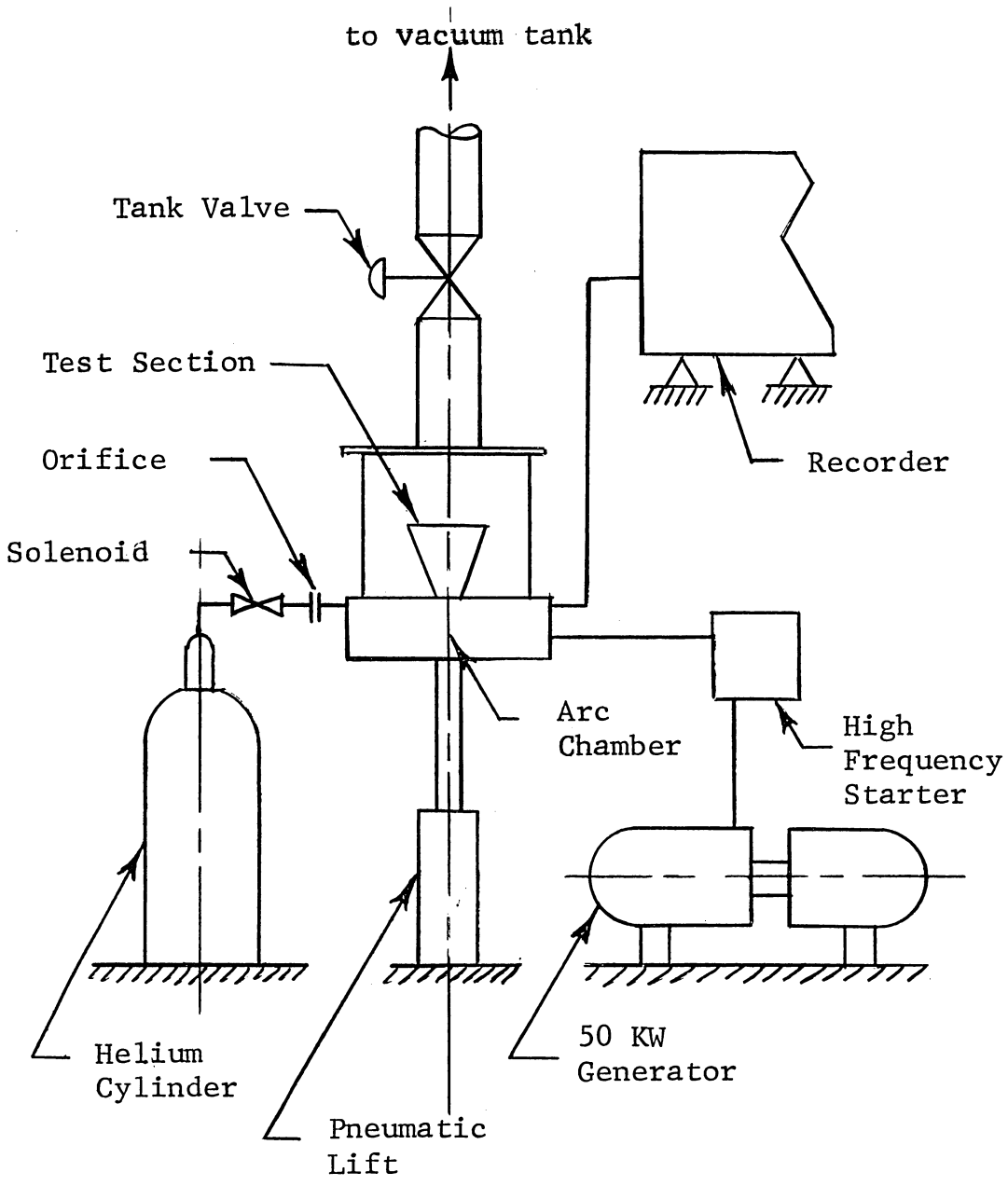

GENERAL SCHEMATIC DRAWING OF THE APPARATUS

Figure 1

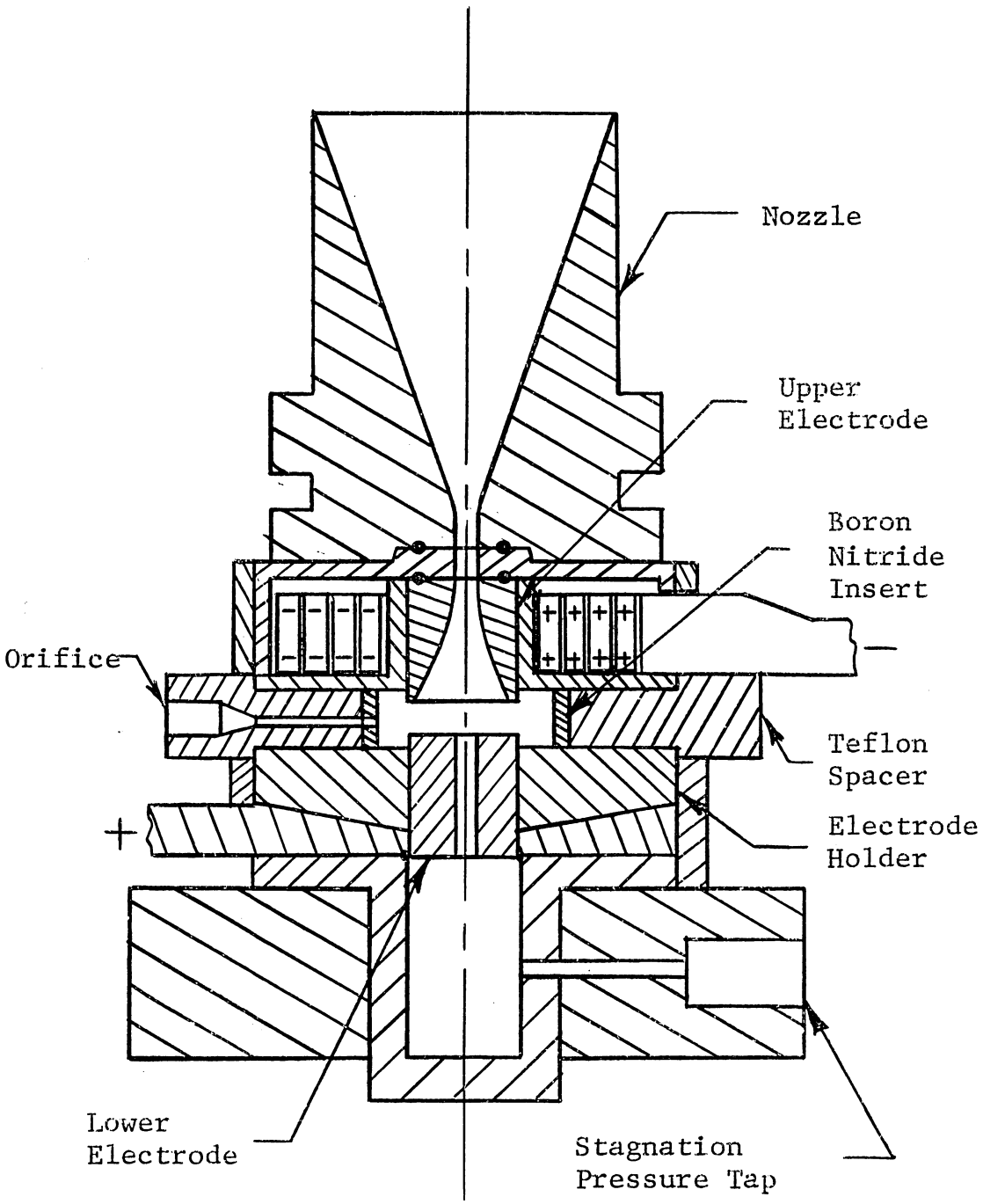
Nozzle
Upper Electrode
Boron Nitride Insert
Orifice
Teflon Spacer
Electrode Holder
Lower Electrode
Stagnation Pressure Tap
ARC CHAMBER

Figure 2

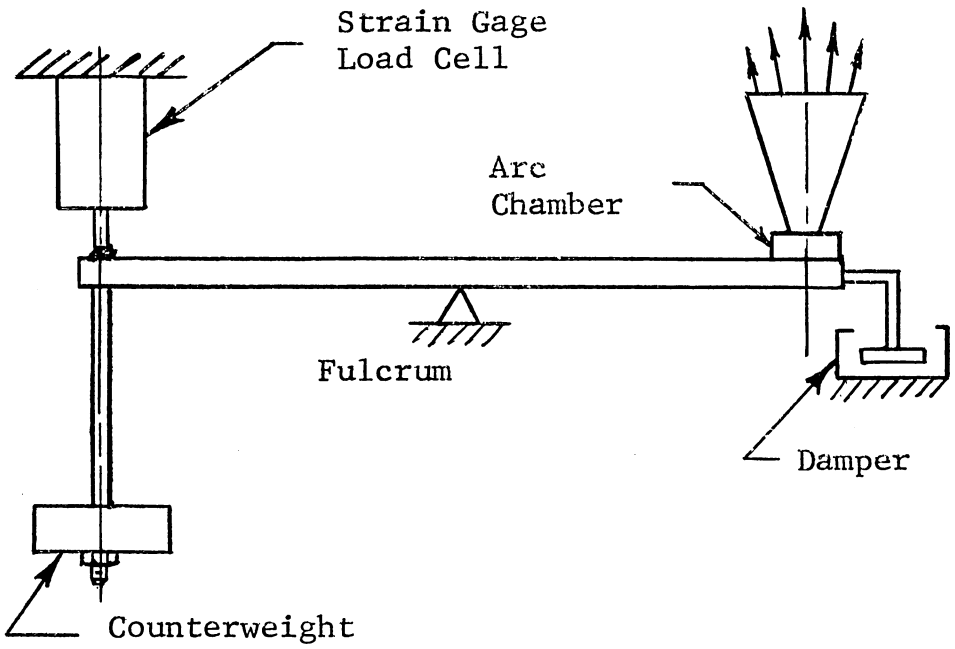

THRUST BALANCE

Figure 3

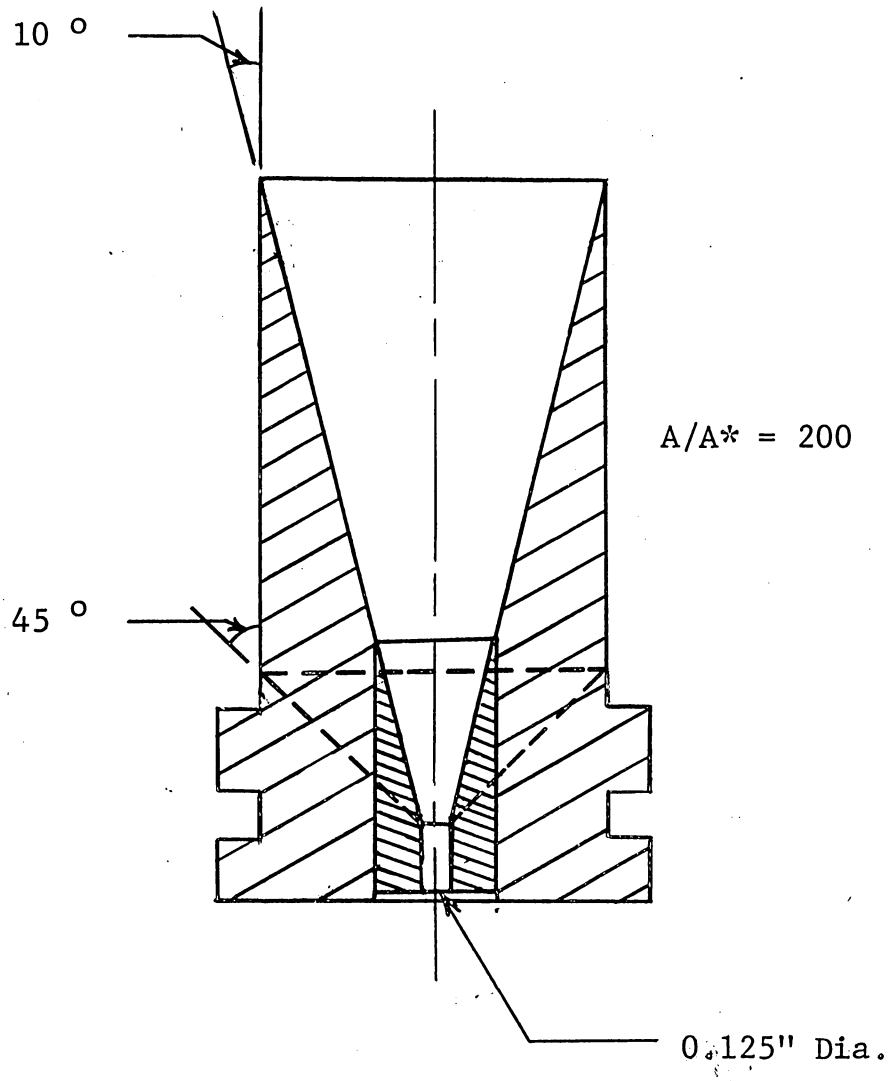

THRUST NOZZLE

Figure 4

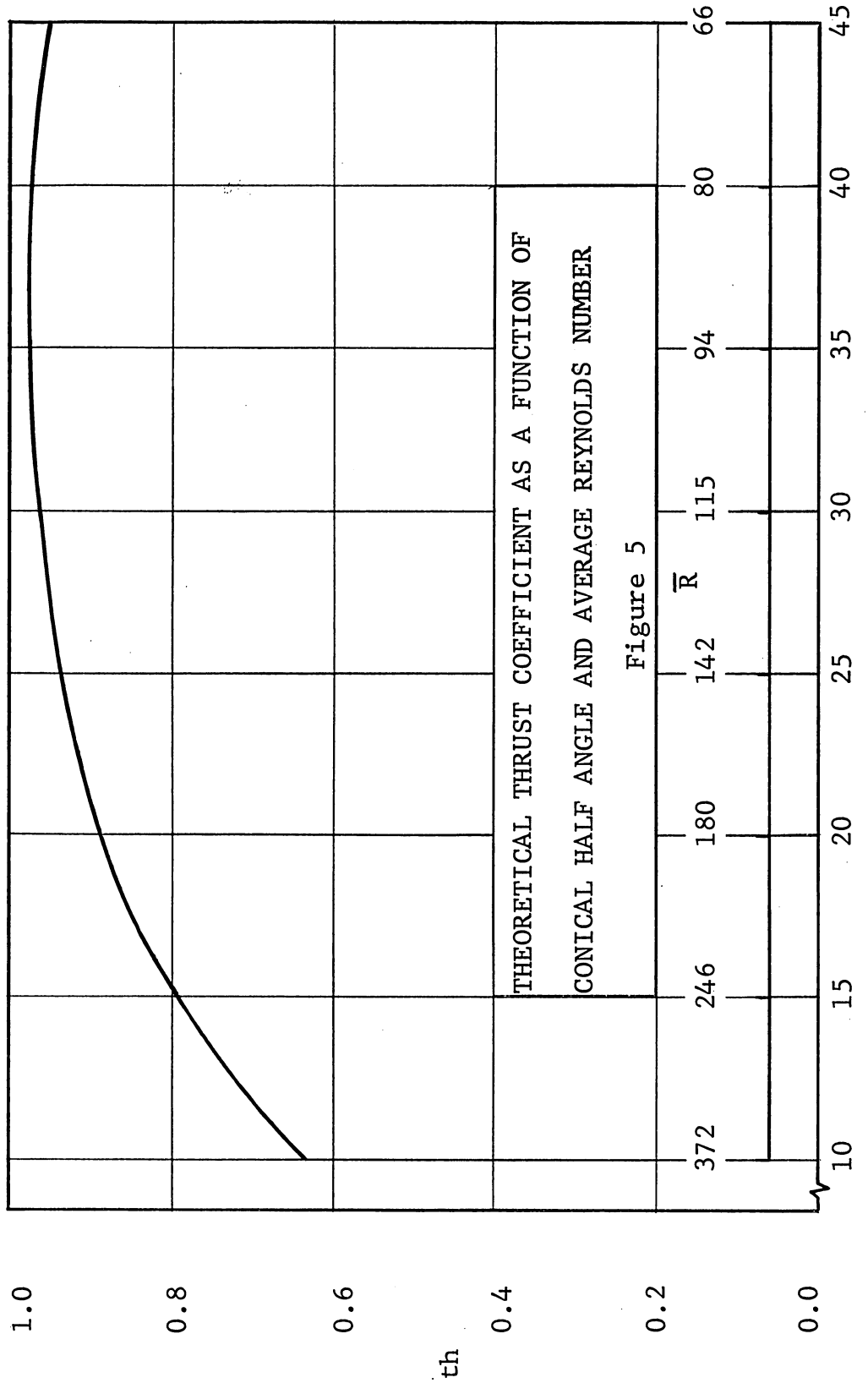

THEORETICAL THRUST COEFFICIENT AS A FUNCTION OF CONICAL HALF ANGLE AND AVERAGE REYNOLDS NUMBER

Figure 5

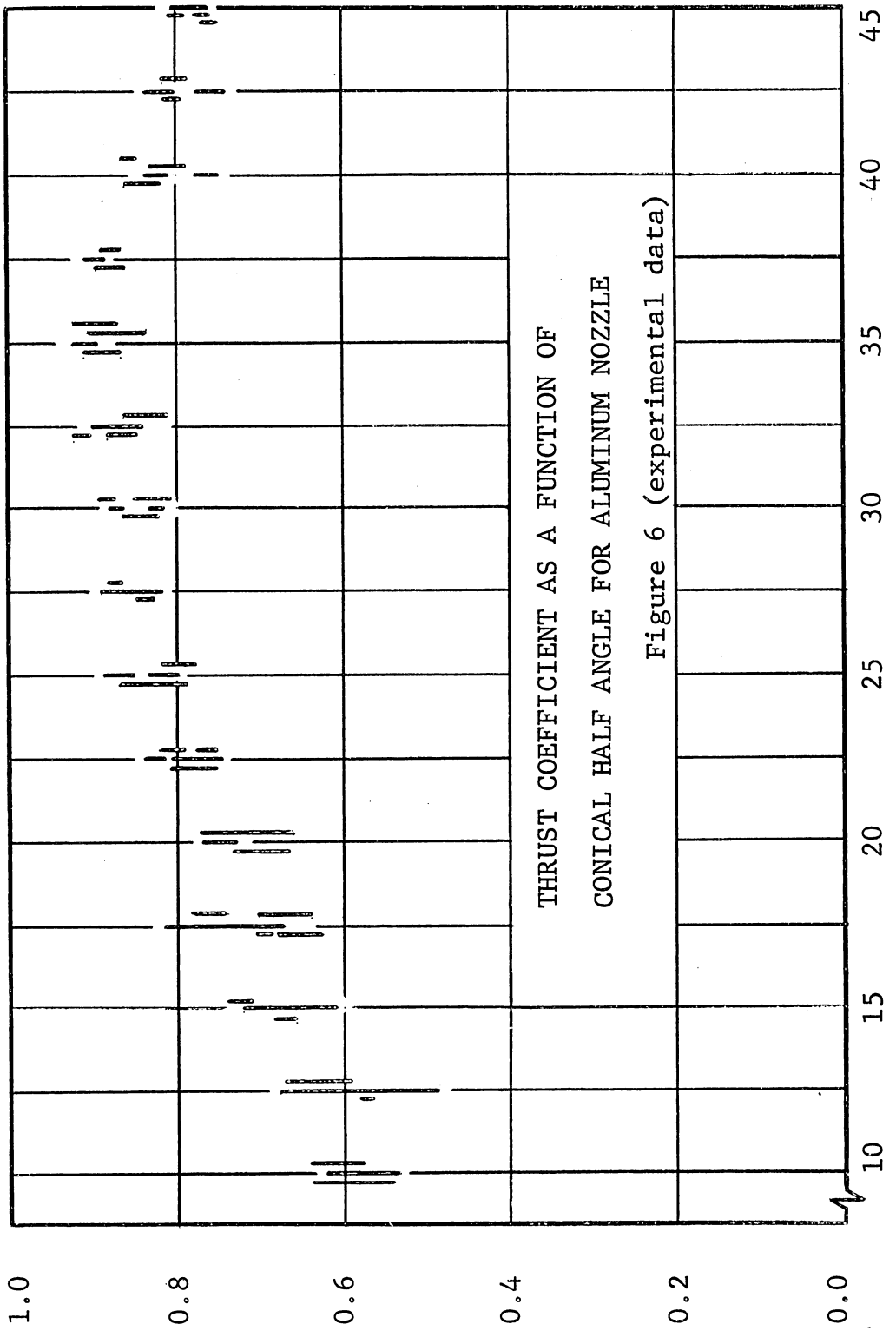
THRUST COEFFICIENT AS A FUNCTION OF
CONICAL HALF ANGLE FOR ALUMINUM NOZZLE
Figure 6 (experimental data)
C_F
1.0
0.8
0.6
0.4
0.2
0.0
10
15
20
25
30
35
40
45
θ degrees

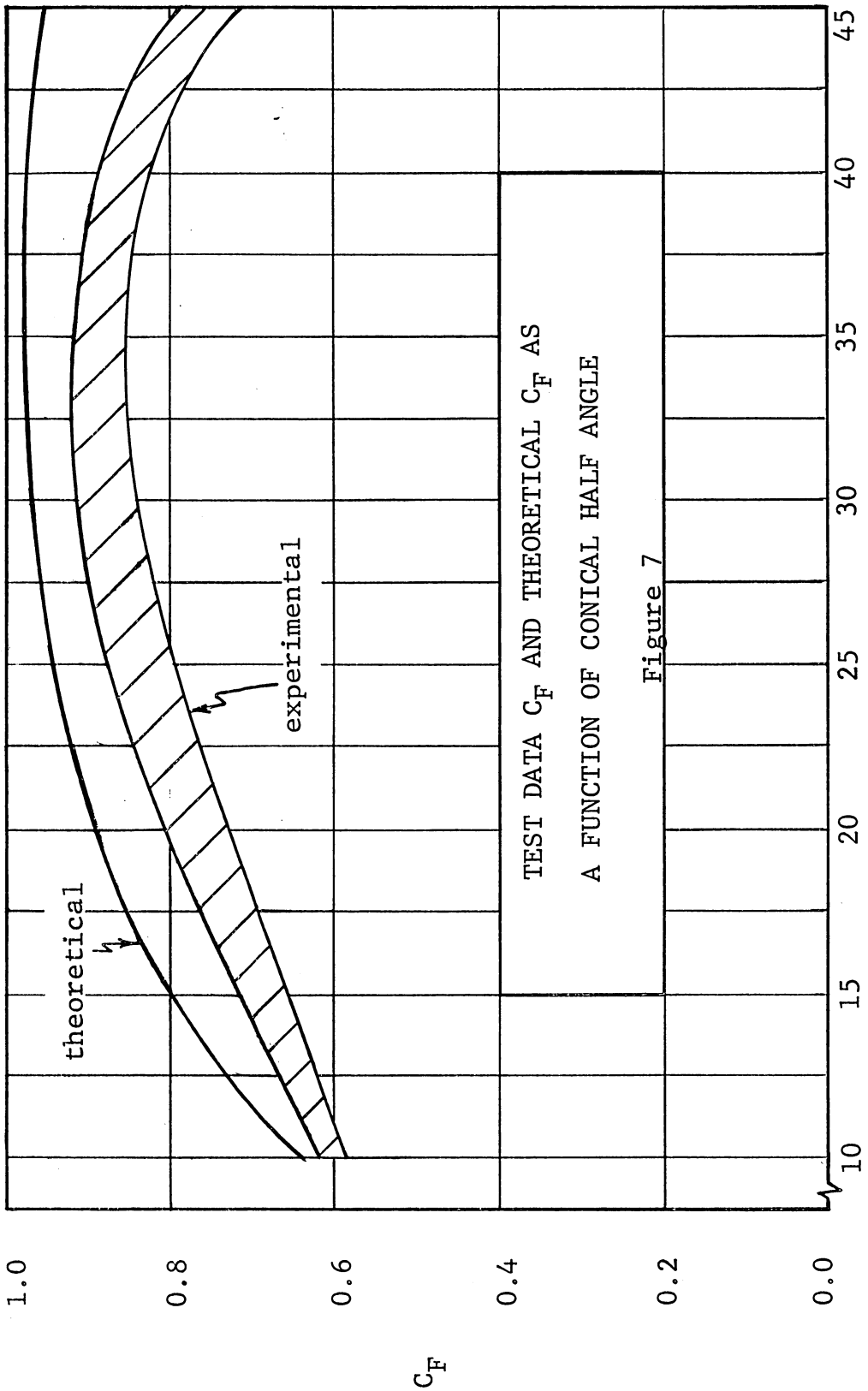

TEST DATA C_F AND THEORETICAL C_F AS A FUNCTION OF CONICAL HALF ANGLE

Figure 7

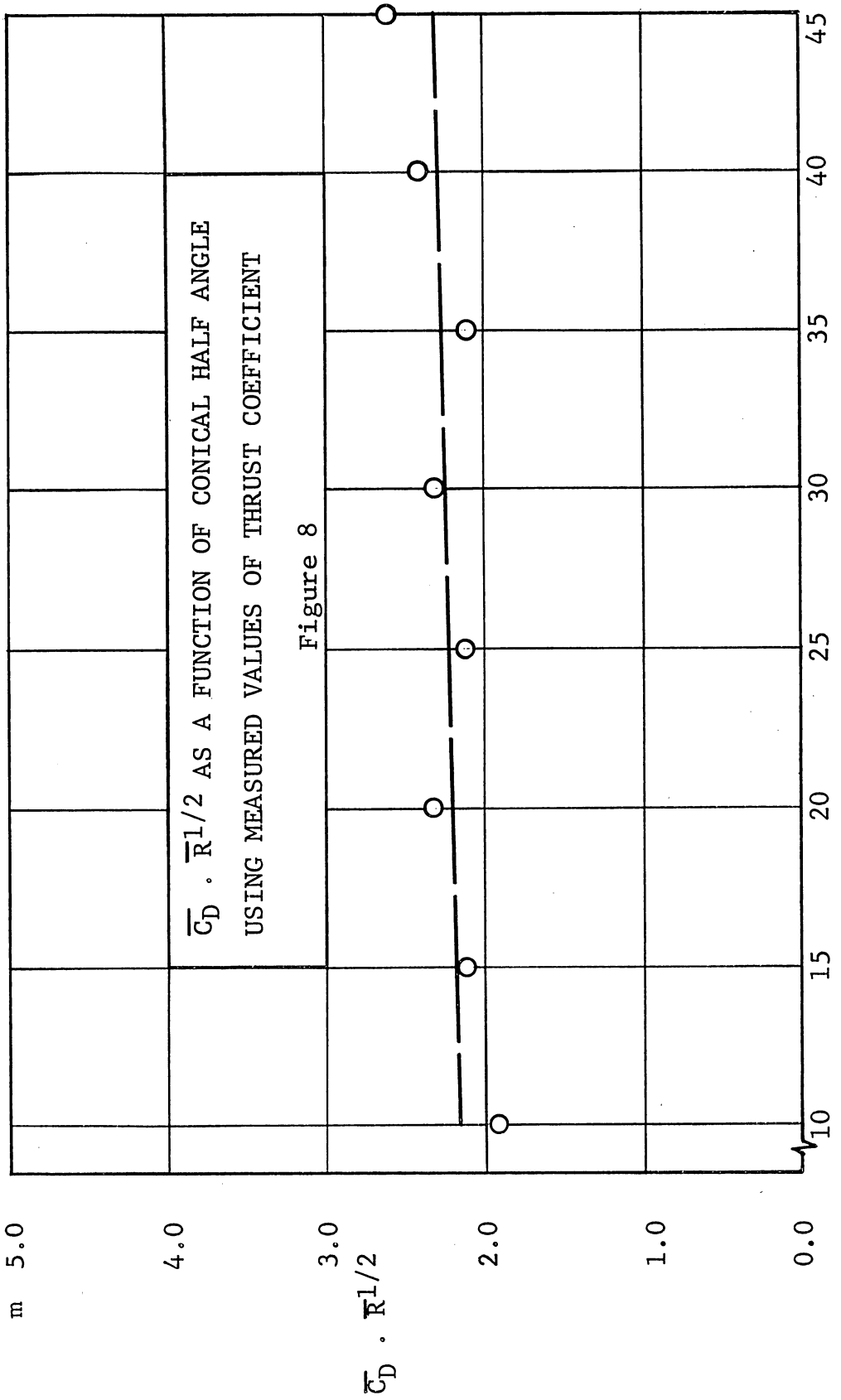
$\overline{C}_D \cdot \overline{R}^{1/2}$ AS A FUNCTION OF CONICAL HALF ANGLE
USING MEASURED VALUES OF THRUST COEFFICIENT
$\overline{C}_D \cdot \overline{R}^{1/2}$
m 5.0
4.0
3.0
2.0
1.0
0.0
10
15
20
25
30
35
40
45
θ degrees

Figure 8

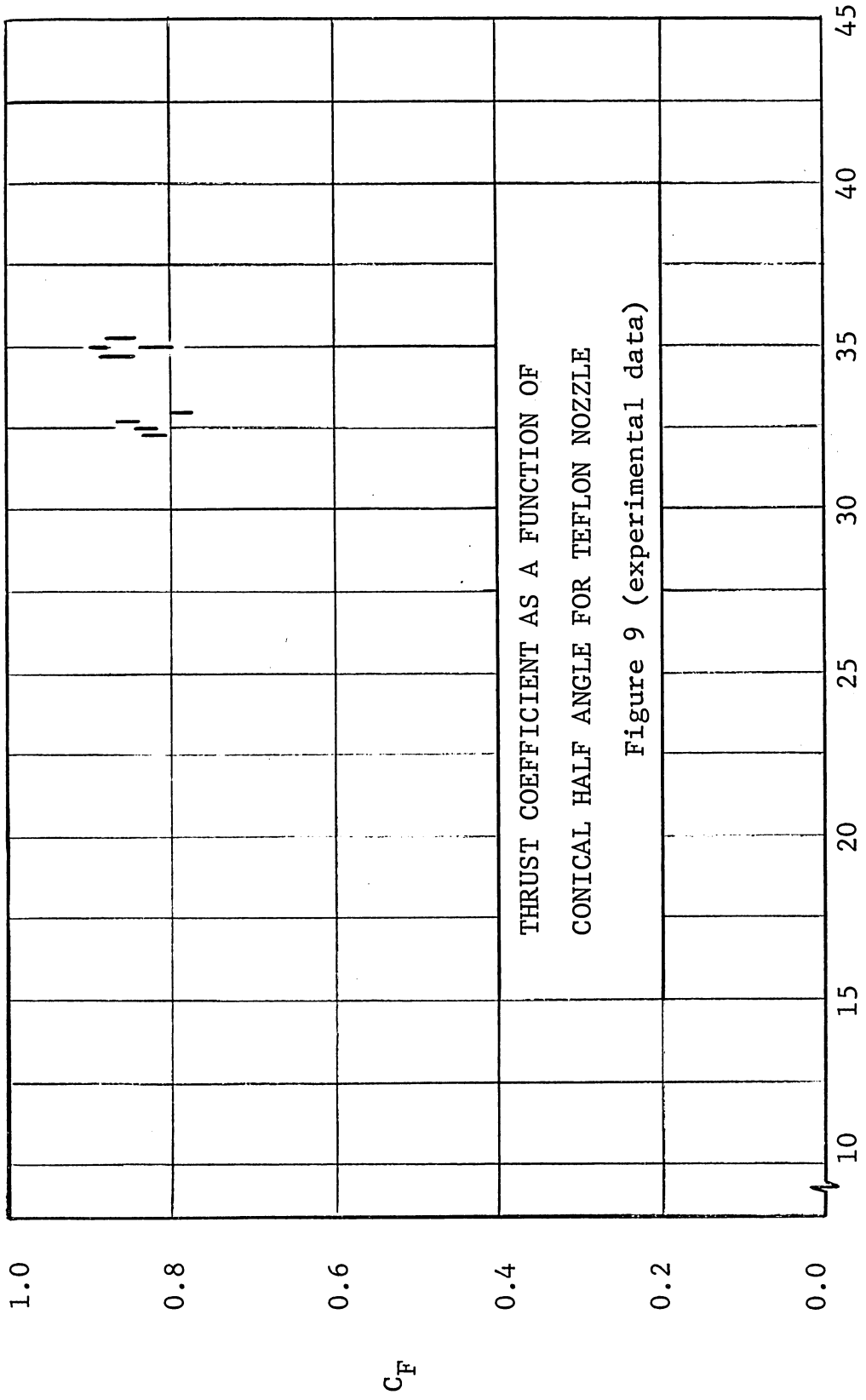

THRUST COEFFICIENT AS A FUNCTION OF
CONICAL HALF ANGLE FOR TEFLON NOZZLE
Figure 9 (experimental data)